

Participant-spectator matter and thermalization of neutron-rich systems at the energy of vanishing flow

Sakshi Gautam and Rajeev K. Puri*

Department of Physics, Panjab University, Chandigarh 160014, India

(Received 20 April 2012; revised manuscript received 16 May 2012; published 12 June 2012)

We present the results of participant-spectator matter at the energy of vanishing flow for neutron-rich systems. Our study reveals similar behavior of the participant-spectator for neutron-rich systems as had been reported for the stable systems and also points towards nearly mass independent behavior of the participant-spectator matter for neutron-rich systems at the energy of vanishing flow. We also study the thermalization reached in the reactions of neutron-rich systems in terms of anisotropy ratio. A nearly mass independent results are also obtained for the anisotropy ratio.

DOI: [10.1103/PhysRevC.85.067601](https://doi.org/10.1103/PhysRevC.85.067601)

PACS number(s): 25.75.Ld, 21.65.Cd, 24.10.Cn

Collective flow has been a boom since it was found to be very sensitive towards various reaction parameters [1,2]. At the same time, it also helped all the way to constrain experimental uncertainties and theoretical degrees of freedom. At low incident energies, the dominance of the mean field leads to attractive (negative) collective transverse flow which turns positive at higher incident energies due to the dominance of nucleon-nucleon scattering. While going from the low to high incident energies, collective flow, therefore, vanishes at a particular incident energy labeled as the energy of vanishing flow (EVF) [3]. The EVF has been reported to scale with the total mass of the colliding pair [4,5]. Unfortunately, various model ingredients, such as the different equations of state (EOS), momentum dependence of the EOS, as well as the nature of the binary collisions, are, therefore, found to affect the energy of vanishing flow, thus leading to different predictions. At the same time, the balancing act of the mean field and nucleon-nucleon scattering at the energy of vanishing flow should also be reflected in other quantities.

Recently, one of us and collaborators analyzed the participant-spectator matter at the energy of vanishing flow and, very interestingly, found that the normalized participant matter (or spectator matter) at the energy of vanishing flow was the same for all colliding pairs [6]. This was not surprising since the above counterbalancing will be directly reflected in participant-spectator matter. Further investigations found it to be insensitive toward different equations of state as well as the momentum dependence of the EOS and, therefore, advocated participant-spectator matter as a barometer for studying the EVF and justified the role of the mean field and nucleon-nucleon scattering at the energy of vanishing flow [6]. The above study was performed for the experimentally measured systems which are stable in nature. On the other hand, recent interest in the study of flow has shifted towards the neutron or proton rich nuclei. Whether it is fusion, cluster radioactivity, or heavy-ion collisions at intermediate energies, one is interested for the matter far from the line of stability. Extensive study has been carried out to pin down the isospin effects via collective flow. In view of these recent developments, one is interested

to see whether the above participant-spectator matter picture is valid for neutron-rich colliding nuclei or not. Therefore, the aim of the present paper is to analyze the participant-spectator matter and thermalization for neutron-rich colliding nuclei at their respective energies of vanishing flow and to see whether the addition of neutron content alters the above reported trends or not. Since this study needs proper implementation of the isospin dynamics, we performed this study with the isospin-dependent quantum molecular dynamics (IQMD) model [7].

In IQMD model, baryons are represented by Gaussian-shaped density distributions [7]

$$f_i(\vec{r}, \vec{p}, t) = \frac{1}{\pi^2 \hbar^2} \exp\left(-[\vec{r} - \vec{r}_i(t)]^2 \frac{1}{2L}\right) \times \exp\left(-[\vec{p} - \vec{p}_i(t)]^2 \frac{2L}{\hbar^2}\right). \quad (1)$$

These hadrons propagate using the Hamilton equations of motion:

$$\frac{d\vec{r}_i}{dt} = \frac{d\langle H \rangle}{d\vec{p}_i}, \quad \frac{d\vec{p}_i}{dt} = -\frac{d\langle H \rangle}{d\vec{r}_i}, \quad (2)$$

with

$$\begin{aligned} \langle H \rangle &= \langle T \rangle + \langle V \rangle \\ &= \sum_i \frac{p_i^2}{2m_i} + \sum_i \sum_{j>i} \int f_i(\vec{r}, \vec{p}, t) V^{ij}(\vec{r}', \vec{r}) \\ &\quad \times f_j(\vec{r}', \vec{p}', t) d\vec{r}' d\vec{r}' d\vec{p}' d\vec{p}'. \end{aligned} \quad (3)$$

The baryon potential V^{ij} , in the above relation, reads as

$$\begin{aligned} V^{ij}(\vec{r}' - \vec{r}) &= V_{\text{Skyrme}}^{ij} + V_{\text{Yukawa}}^{ij} + V_{\text{Coul}}^{ij} + V_{\text{Sym}}^{ij} \\ &= \left[t_1 \delta(\vec{r}' - \vec{r}) + t_2 \delta(\vec{r}' - \vec{r}) \rho^{\gamma-1} \left(\frac{\vec{r}' + \vec{r}}{2} \right) \right] \\ &\quad + t_3 \frac{\exp(|\vec{r}' - \vec{r}|/\mu)}{|\vec{r}' - \vec{r}|/\mu} + \frac{Z_i Z_j e^2}{|\vec{r}' - \vec{r}|} \\ &\quad + t_4 \frac{1}{\rho_0} T_{3i} T_{3j} \delta(\vec{r}'_i - \vec{r}'_j). \end{aligned} \quad (4)$$

Here $t_4 = 4C$ with $C = 32$ MeV, Z_i and Z_j denote the charges of the i th and j th baryon, and T_{3i} and T_{3j} are their respective T_3 components (i.e., $1/2$ for protons and $-1/2$ for

* rkpuri@pu.ac.in

neutrons). For the density dependence, standard Skyrme-type parametrization is employed.

For the present analysis, we simulated the reactions of Ca + Ca, Ni + Ni, Zr + Zr, Sn + Sn, and Xe + Xe series having neutron-proton ratios (N/Z) \sim 1.0, 1.6, and 2.0. We define a quantity, Iso_{fac} [$= N/Z - 1$], which represents the increase in the neutron content with respect to symmetric systems. For symmetric systems (having equal numbers of protons and neutrons) $Iso_{fac} = 0$ and it increases with the increase in the neutron content of the colliding system. In particular, we simulated the reactions of $^{40}\text{Ca} + ^{40}\text{Ca}$, $^{52}\text{Ca} + ^{52}\text{Ca}$, $^{60}\text{Ca} + ^{60}\text{Ca}$; $^{56}\text{Ni} + ^{56}\text{Ni}$, $^{72}\text{Ni} + ^{72}\text{Ni}$, $^{84}\text{Ni} + ^{84}\text{Ni}$; $^{81}\text{Zr} + ^{81}\text{Zr}$, $^{104}\text{Zr} + ^{104}\text{Zr}$, $^{120}\text{Zr} + ^{120}\text{Zr}$; $^{100}\text{Sn} + ^{100}\text{Sn}$, $^{129}\text{Sn} + ^{129}\text{Sn}$, $^{150}\text{Sn} + ^{150}\text{Sn}$; and $^{110}\text{Xe} + ^{110}\text{Xe}$, $^{140}\text{Xe} + ^{140}\text{Xe}$, $^{162}\text{Xe} + ^{162}\text{Xe}$ at an impact parameter $b/b_{\text{max}} = 0.2\text{--}0.4$ using a soft EOS along with the standard isospin- and energy-dependent cross section reduced by 20%, i.e., $\sigma = 0.8\sigma_{\text{nn}}^{\text{free}}$ at several incident energies between 60 and 105 MeV/nucleon. The collective flow and EVF was then calculated using the procedure reported in Refs. [5,8]. The corresponding energies of vanishing flow for the above colliding pairs are, respectively, 105, 85, 73; 98, 82, 72; 86, 74, 67; 82, 72, 64; and 76, 68, 61 MeV/nucleon. As noted, in agreement with the previous studies, the EVF decreases for larger neutron content [9]. This decrease was found to be due to the mass effects as well as isospin effects.

Since the energy of vanishing flow represents the counterbalancing of the attractive mean field potential and repulsive nucleon-nucleon scattering, one expects that this counterbalancing should also be seen in the participant and

spectator matter as predicted in Ref. [6]. In the present study, participant-spectator matter is defined in terms of the nucleonic concept. All nucleons having experienced at least one collision are counted as *participant matter* scaled to the total mass of the reacting nuclei. The remaining matter is labeled as *spectator matter*. Note that here only those collisions are considered that are cleared by the Pauli principle. Alternatively, as suggested in Ref. [6], one can analyze the participant-spectator matter in terms of various rapidity cuts. As shown in Ref. [6], both the above definitions give same results. The latter quantity can also be deduced experimentally and hence our predictions can also be verified. These definitions give us the possibility to analyze the reaction in terms of the participant-spectator fireball model. This concept gives similar results as has been demonstrated in the fireball model of Gosset *et al.* [10].

In Fig. 1, we display the time evolution of spectator matter and participant matter. The upper panels represent the results of spectator and participant matter for $Iso_{fac} = 0$, whereas the left and right lower panels represent results of participant matter for $Iso_{fac} = 0.6$ and 1.0, respectively. Lines correspond to different systems. Solid, dashed, dotted, dash-dotted, and short-dotted lines represent the reactions of Ca + Ca, Ni + Ni, Zr + Zr, Sn + Sn, and Xe + Xe, respectively. It is trivial to note that the entire matter is spectator at the beginning but it turns participant with the passage of time. We also find that for lighter systems like Ca + Ca and Ni + Ni, the transition from the spectator to participant matter is swift and sudden whereas for the heavier colliding nuclei, the transition is slow and gradual. This happens because of the fact that the EVF for lighter reactions is higher compared to heavy nuclei. We

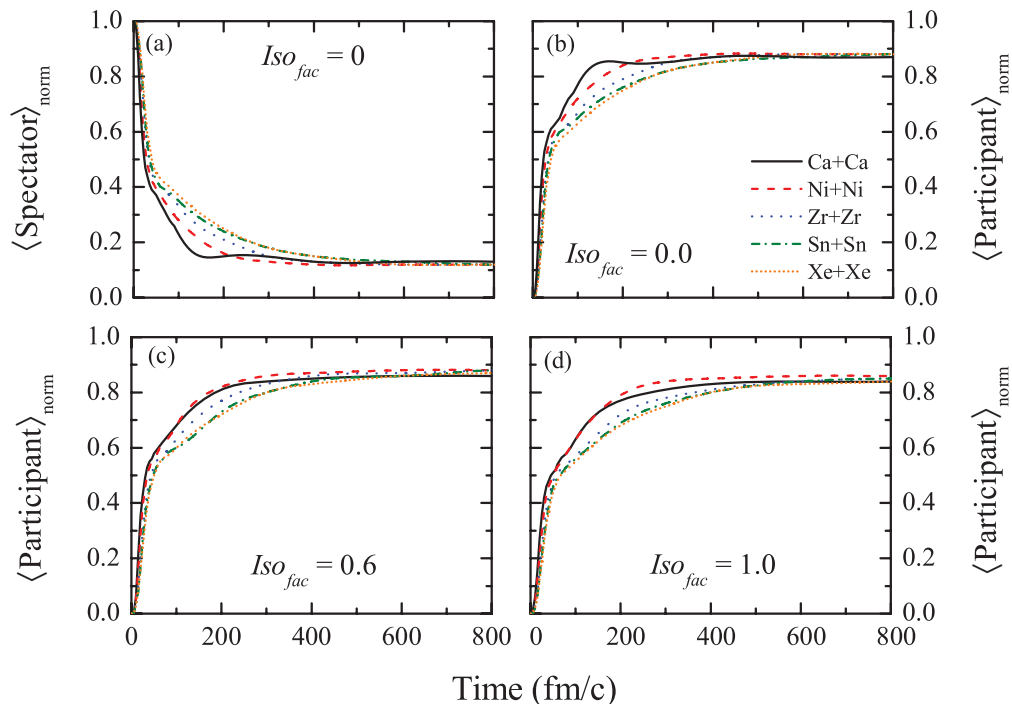


FIG. 1. (Color online) The time evolution of (a) spectator matter and (b), (c), (d) participant matter for the colliding pairs having $Iso_{fac} = 0, 0.0, 0.6,$ and 1.0 . Lines are explained in the text.

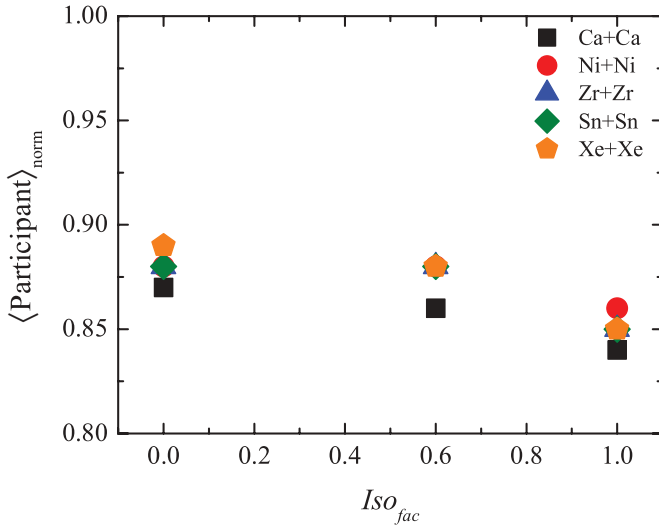


FIG. 2. (Color online) The normalized participant matter as a function of Iso_{fac} . Symbols are explained in the text. Here analysis is made at corresponding energies of vanishing flow.

also see a similar behavior for all N/Z ratios. This indicates that participant-spectator behavior is similar for neutron-rich systems as for systems lying on the stability line ($N/Z = 1$).

In Fig. 2, we display the participant matter as a function of Iso_{fac} . Squares, circles, triangles, diamonds, and pentagons represent the reactions of Ca + Ca, Ni + Ni, Zr + Zr, Sn + Sn, and Xe + Xe, respectively. We find that for all the systems, the participant matter is almost independent of the neutron

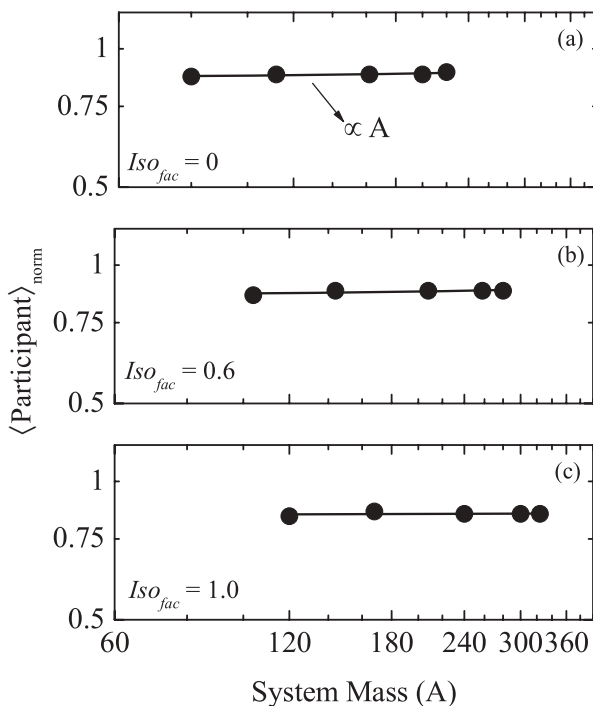


FIG. 3. The system size dependence of the normalized participant matter obtained at the final stage for different Iso_{fac} . All reactions were performed at their corresponding EVF. Lines represent a linear fit ($\propto A$).

content. As a result, normalized spectator matter will also be independent of neutron content.

In Fig. 3, we display the system size dependence of the participant matter at the energy of vanishing flow. Symbols represent participant matter. Upper, middle, and lower panels represent the results for $Iso_{\text{fac}} = 0, 0.6$, and 1.0 , respectively. We see that participant matter (alternatively, the spectator matter) follows a linear behavior $\propto A$, the system mass. The slope is almost zero that makes the behavior nearly mass independent. A nearly mass independent behavior is obeyed by the participant (and spectator matter) for all the N/Z ratios. From the above analysis, it is clear that no effect of neutron content is visible on the participant-spectator matter.

It has been known that participant-spectator matter also acts as an indicator for thermalization. For the deeper understanding, we analyze the thermalization with different definitions. In Fig. 4, we display the time evolution of the anisotropy ratio $\langle R_a \rangle$ (upper panel) and the relative momentum $\langle K_R \rangle$ (lower panel) for different system masses having $Iso_{\text{fac}} (N/Z) = 0 (1.0)$. The $\langle R_a \rangle$ is defined as [11]

$$\langle R_a \rangle = \frac{\sqrt{p_x^2} + \sqrt{p_y^2}}{2\sqrt{p_z^2}}. \quad (5)$$

This anisotropy ratio is an indicator of the global equilibrium of the system. This represents the equilibrium of the

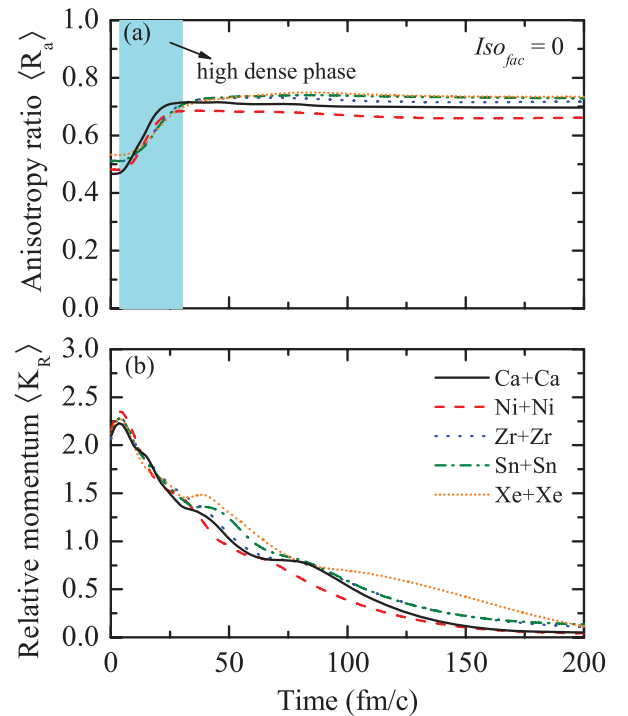


FIG. 4. (Color online) The time evolution of the anisotropy ratio $\langle R_a \rangle$ (upper panel) and relative momentum $\langle K_R \rangle$ (lower panel) for various systems having $Iso_{\text{fac}} = 0$. Lines have the same meaning as in Fig. 1. Analysis is made at the corresponding EVF. Shaded portion represents the high density phase of the reaction (corresponding to $\rho/\rho_0 > 1.0$).

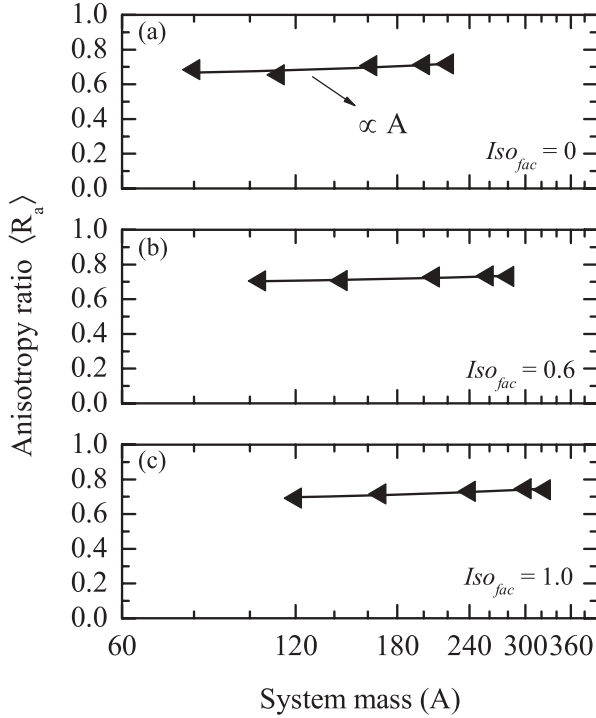


FIG. 5. The system size dependence of the anisotropy ratio $\langle R_a \rangle$ for various Iso_{fac} . All results correspond to the EVF and analysis is made at final stages.

whole system and does not depend on the local positions. The full global equilibrium averaged over a large number of events will correspond to $\langle R_a \rangle = 1$. The second quantity, the relative momentum $\langle K_R \rangle$ of two colliding Fermi spheres, is defined as [11]

$$\langle K_R \rangle = \langle |\vec{P}_P(\vec{r}, t) - \vec{P}_T(\vec{r}, t)| \rangle, \quad (6)$$

where

$$\vec{P}_i(\vec{r}, t) = \frac{\sum_{j=1}^A \vec{P}_j(t) \rho_j(\vec{r}, t)}{\rho_j(\vec{r}, t)}, \quad i = 1, 2. \quad (7)$$

Here \vec{P}_j and ρ_j are the momentum and density of the j th particle and i stands for either a projectile or target. As noted,

this quantity measures deviation from a single Fermi sphere and hence represents local equilibrium. It is worth mentioning that such a concept of local equilibrium is commonly used in the hydrodynamical model. Obviously, with the passage of the time, density in a central sphere will decrease due to lesser and lesser nucleons and, as a result, $\langle K_R \rangle$ will also decrease. On the other hand, no such density dependence exists for $\langle R_a \rangle$. The anisotropy ratio $\langle R_a \rangle$ will saturate after the finishing of the reaction.

From Fig. 4(a) (upper panel), we see that anisotropy ratio increases as the reaction proceeds and finally saturates after the high density phase is over. We also note an insignificant influence of the system size on the anisotropy ratio indicating equilibration of the system. From Fig. 4(b) (lower panel) we see that the relative momentum decreases as the reaction proceeds. Smaller values of $\langle K_R \rangle$ at the end of the reaction indicates better local thermalization of the matter. We also see from the figure that the $\langle R_a \rangle$ ratio saturates as soon as the high density phase is over that signifies that the nucleon-nucleon collisions happening after the high density phase do not change the momentum space significantly. This figure indicates how global and local equilibrium are reached in various reactions at the energy of vanishing flow.

In Fig. 5, we display the system size dependence of the anisotropy ratio for systems having $Iso_{fac} = 0, 0.6$, and 1.0 . From the figure, we see that anisotropy ratio follows a linear behavior $\propto A$, the system size. The values of various slopes are almost zero indicating a mass independent nature.

In summary, we studied the participant-spectator matter at the energy of vanishing flow for neutron-rich systems. The study revealed a similar behavior of the participant-spectator for neutron-rich systems as was reported for stable systems and points towards a nearly mass independent behavior of participant-spectator matter of neutron-rich systems at the energy of vanishing flow. Similar mass independent behavior is also found for the anisotropy ratio.

This work has been supported by a grant from Center of Scientific and Industrial Research (CSIR), government of India, and Indo-French Center for the Promotion of Advanced Research (IFCPAR) under Project No. 4104-1.

- [1] A. Andronic *et al.*, *Phys. Rev. C* **67**, 034907 (2003); Y. Zhang and Z. Li, *ibid.* **74**, 014602 (2006).
 [2] B. Hong *et al.*, *Phys. Rev. C* **66**, 034901 (2006).
 [3] D. Krofcheck, W. Bauer, G. M. Crawley, C. Djalali, S. Howden, C. A. Ogilvie, A. Vander Molen, G. D. Westfall, W. K. Wilson, R. S. Tickle, and C. Gale, *Phys. Rev. Lett.* **63**, 2028 (1989).
 [4] G. D. Westfall *et al.*, *Phys. Rev. Lett.* **71**, 1986 (1993).
 [5] A. D. Sood and R. K. Puri, *Phys. Rev. C* **69**, 054612 (2004).
 [6] A. D. Sood and R. K. Puri, *Phys. Rev. C* **70**, 034611 (2004); **79**, 064618 (2009).
 [7] C. Hartnack, Rajeev K. Puri, J. Aichelin, J. Konopka, S. A. Bass, H. Stocker, and W. Greiner, *Eur. Phys. J. A* **1**, 151 (1998).
 [8] S. Gautam, A. D. Sood, R. K. Puri, and J. Aichelin, *Phys. Rev. C* **83**, 014603 (2011).
 [9] S. Gautam, R. Chugh, A. D. Sood, R. K. Puri, C. Hartnack, and J. Aichelin, *J. Phys. G: Nucl. Part. Phys.* **37**, 085102 (2010); B. A. Li, Z. Ren, C. M. Ko, and S. J. Yennello, *Phys. Rev. Lett.* **76**, 4492 (1996); R. Pak, Bao-An Li, W. Benenson, O. Bjarki, J. A. Brown, S. A. Hannuschke, R. A. Lacey, D. J. Magestro, A. Nadasen, E. Norbeck, D. E. Russ, M. Steiner, N. T. B. Stone, A. M. Vander Molen, G. D. Westfall, L. B. Yang, and S. J. Yennello, *ibid.* **78**, 1026 (1997).
 [10] J. Gosset, H. H. Gutbrod, W. G. Meyer, A. M. Poskanzer, A. Sandoval, R. Stock, and G. D. Westfall, *Phys. Rev. C* **16**, 629 (1977).
 [11] D. T. Khoa, N. Ohtsuka, M. A. Matin, A. Faessler, S. W. Huang, E. Lehmann, and Rajeev K. Puri, *Nucl. Phys. A* **548**, 102 (1992); Rajeev K. Puri, N. Ohtsuka, E. Lehmann, Amand Faessler, M. A. Matin, Dao T. Khoa, G. Batko, and S. W. Huang, *ibid.* **575**, 733 (1994).